Author Accepted Manuscript

Accepted for publication 7 October 2019

Multicomponent bulk metallic glasses with elevated-temperature resistance

A. Inoue[1-4*], F.L. Kong[2], S.L. Zhu[4] and A.L. Greer[5*]

Metallic glasses have attractive properties, but as the glassy state is inherently metastable, they are not normally considered for application at elevated temperatures. Yet, studies have shown that multicomponent and pseudo high-entropy (PHE) compositions can confer useful heat resistance. The formation, thermal stability, and mechanical and chemical properties of multicomponent Fe-(Cr,Mo)- and Zr-based bulk metallic glasses (BMGs) are reviewed to assess their potential as structural heat-resistant materials. The composition $Fe_{43}Cr_{16}Mo_{16}C_{15}B_{10}$ is castable fully glassy with rod diameters up to 4 mm; glassy coatings with low porosity, and with good mechanical properties and good corrosion resistance, can be produced by high-velocity spray-coating. The compositions $Zr_{55–65}Al_{7.5–10}(TM_1,TM_2)_{27.5–35}$ (TM_1 = Fe,Co,Ni, TM_2 = Cu,Pd,Ag,Au) give PHE BMGs, in which a stable cluster-like glassy phase without crystalline precipitates is formed by annealing at temperatures well above the first calorimetric transformation. It is suggested that proliferation of alloy components is an effective method to synthesize metastable metallic materials that retain high strength at elevated temperatures.

Keywords: amorphous; phase transformation; strength; coating; corrosion

1. Introduction

Most of the common metals have a simple crystal structure: body-centered cubic (bcc), face-centered cubic (fcc) or hexagonal closed-packed (hcp), though their alloys may include compounds with more complex structures. It is of interest to synthesize novel alloys with different structures that may be expected to

give unique and useful properties. One effective method to change structures is alloying with more metallic elements; this can change the structure from crystalline to glassy even in a cast bulk form [1–3]. The formation of a bulk metallic glass (BMG) is associated with alloys in which the selection of components follows three rules, namely: (1) at least three elemental components, (2) significant atomic size mismatches above 12% among the main three elements, and (3) negative heats of mixing among the three elements [1, 4]. In addition, such multicomponent alloys have deep eutectic valleys and permit access to a highly supercooled liquid state, resulting in the formation of BMGs which have an atomic configuration that is disordered at long range and ordered at a medium range of 1.7–2.0 nm [5]. These BMGs exhibit unique combinations of properties that cannot be obtained for crystalline alloys, e.g., ultra-high strength, large elastic strain, high corrosion resistance, high wear resistance, surface smoothness, viscous flowability, net castability and precise formability [1, 4]. In addition, Fe- and Co-based BMGs exhibit good soft magnetic properties with low coercivity, high permeability and low core loss because their atomic configuration is uniform on the scale of magnetic domains [1, 4]. Exploiting these advantages, BMGs have been used in many fields such as structural, soft-magnetic, coatings, ornamental, casing, spring, sensor, mirror, gear, hinge, bolt, cutlery etc. [1, 4]

In general BMGs have compositions selected to optimize their glass-forming ability (GFA). In addition to these, an equiatomic multicomponent BMG was synthesized for $Ti_{20}Zr_{20}Hf_{20}Ni_{20}Cu_{20}$ in 2002 [6]. Two years later, equiatomic multicomponent crystalline alloys with fcc and bcc structures were also formed for $Fe_{20}Co_{20}Ni_{20}Cr_{20}Mn_{20}$ [7] and $Al_{20}Fe_{20}Co_{20}Ni_{20}Cr_{20}$ [8] , respectively. The latter was named as a high-entropy (HE) alloy in the paper. Since these syntheses, much attention has been paid to equiatomic and near-equiatomic multicomponent alloys, because these show metastable supersaturated solid solution (SSSS) phases with bcc and fcc structures in the absence of compounds, or show a glassy structure [9, 10]. Subsequently, pseudo-high entropy (PHE) glassy alloys, where the definition is different from HE alloys, have been synthesized [11–13]. The PHE type $Zr_{55–65}Al_{7.5–10}(TM_1,TM_2)_{27.5–35}$ (TM_1 = Fe, Co, Ni, TM_2=Cu, Ag, Pd, Au) glassy alloys exhibit

a novel phase decomposition leading to the formation of a cluster-like glassy structure.

This paper aims to review the formation, thermal stability, mechanical and chemical properties and applications of multicomponent Fe- and PHE Zr-based BMGs with a high resistance to phase decomposition and to investigate the usefulness of these BMGs as heat-resistant materials.

2. Development of amorphous alloy steels

Alloy steels containing Cr and Mo are well known as low-cost heat-resistant materials. Since the first synthesis of an amorphous alloy (in the Au-Si system) by rapid solidification in 1960 [14], amorphous alloys have attracted significant attention as potential novel advanced materials. The metastable nature of amorphous or glassy alloys, however, makes them not obvious as heat-resistant materials. When considering possible heat-resistant amorphous alloys for structural applications, Fe-based systems with similar alloy components as in conventional heat-resistant materials are attractive as precursor materials. In the development of structural Fe-based amorphous alloys, Fe-(Cr,Mo,W)-C ternary and quaternary amorphous alloys were synthesized by rapid solidification in 1978 [15–17]. Among these, $Fe_{82-x-y}Cr_xMo_yC_{18}$ alloys had a wide amorphous composition range of 0–50 at% Cr and 0–26 at% Mo and were named as amorphous alloy steels. These amorphous steels exhibit a high crystallization temperature (T_x) of 490–660 K, good bending plasticity, high tensile fracture strength of 3450–3790 MPa, high Vickers hardness (H_v) of 910–1130, and high corrosion resistance in various solutions. There is a clear tendency for T_x and H_v to increase with increasing Cr and Mo contents. In scanning calorimetry, these alloys do not show a glass transition and have been termed amorphous-type alloys. The absence of a detectable glass transition, reflects the instability of the supercooled liquid (SL) state and shows that these systems do not have a high GFA.

Much effort was made to develop a highly heat-resistant material by using these amorphous alloy steels as a precursor [18, 19]. These heat-resistant alloys were produced in two simple stages: (1) production of amorphous alloy powders by high-

pressure gas atomization or pulverization of melt-spun amorphous alloy ribbons subjected to annealing-induced embrittlement treatment, followed by (2) uniaxial hot pressing, hot isostatic pressing or spark plasma sintering of the amorphous powders. The resulting press-sintered bulks have high packing densities above 99% and a mixed structure of fine carbides dispersed homogeneously in bcc or tempered martensite matrix phase. The H_v is dependent on the pressing temperature (T_p), showing a maximum near to T_p of 1273 K and decreasing rapidly with further increase of T_p, owing to the grain growth of the constituent phases. Press-sintered bulk alloys of the Fe-Cr-Mo-C and Fe-Cr-Mo-V-C systems were tested as heat-resistant high-speed cutting or bolt materials, and were confirmed to exhibit favorable characteristics [20]. However, no significant applications were realized because of the relatively high cost of these materials.

3. Fe-based BMGs and their applications

In 1995, a breakthrough was made with the synthesis of the first Fe-based BMGs. Multicomponent Fe-(Al,Ga)-(P,B,Si,C) alloys, with compositions following the three rules noted above [21], were made by copper mold casting. These pioneering Fe-based BMGs were, however, not usable as structural materials. Much effort has since been devoted to develop a structural Fe-based BMG on the basis of previous data [15–17] on Fe-(Cr,Mo)-C amorphous alloys. In 2002, new BMGs in the Fe-Cr-Mo-C-B system were synthesized in rod form with diameters up to 2.7 mm by copper mold casting [22]. The glassy phase is formed over a wide composition range of 0–30 at% Cr, 7.5–22.5 at% Mo and a wide concentration ratio range of C/B, as shown in Fig. 1. These BMGs exhibit high T_g (860–940 K), wide SL region (40–90 K), high T_x (900–1010 K) and high corrosion resistance [23]. The high corrosion resistance originates from the spontaneous formation of a thin, highly passive $Cr_x(OH)_y$ surface layer.

The bulk GFA has been significantly improved by adding small amounts of lanthanide elements (Y and Tm), as exemplified by FeCrMoCBY [24], FeCrMoMnCBY [25] and FeCrMoCBTm [26] alloys, shown in Fig. 2; the maximum diameter for glass formation reaches 10 mm for these three alloy systems and 16

mm for the FeCoCrMoCBTm system [26]. The high GFA for these Fe-based alloys has been reported to be related to the development of medium-range-ordered atomic configurations. For example, for FeCrMoCB and FeCrMoCBTm BMGs, these reflect, respectively, the complex structures of cubic $M_{23}(C,B)_6$ and $M_6(C,B)$ [24, 27]. These compounds have large unit cells that include icosahedral-like local atomic configurations. The addition of Ln has been interpreted to cause the formation of denser atomic configurations through greater adherence to the three component rules for the formation of BMGs and stabilization of the SL [27, 28].

Exploiting the high GFA that enables the production of BMGs with diameters above several millimeters, glassy deposits with thickness of 0.2–0.5 mm have been applied over a wide surface area by high velocity oxy-fuel (HVOF) spray coating on to diverse substrates such as stainless steels, plain carbon steels, Al alloys and Mg alloys [29, 30]. Figure 3(a) shows the cross-sectional structure of a Fe-Cr-Mo-C-B glassy coating that is fully dense and has a high compressive strength. The coating has good corrosion resistance (Fig. 3(b)). There is no appreciable exfoliation of the coating from the substrate for samples subjected to repeated bending deformation (JIS test, Fig. 3(c)). Figure 3(d) shows coatings applied on pipes. The coating shows excellent wear resistance exceeding that of commercial CrN coatings and hard chromium plating (Table 1). The Fe-Cr-Mo-B glassy coating has found application, because its combination of favorable properties cannot be obtained for any crystalline coating. Figure 4 shows an example of the glassy coating on a vessel for the melting of lead-free solder. The elimination of lead increases the temperature required for liquid processing and greatly increases the corrosive attack on the steel vessel. The Fe-Cr-Mo-C-B glassy coating demonstrates retention of corrosion and erosion resistances, and of strength, at elevated temperatures [4]. It can be used for at least 6 months, much longer than the usable life (50 days) of the best-performing stainless steel [30]. The transition to the use of lead-free solder has clear environmental benefits, and the use of the glassy coating facilitates cleaner processing, relevant for sustainability.

4. Zr-based clustered glassy alloys

The primary precipitation phase for $Zr_{65}Al_{7.5}Ni_{10}Cu_{17.5}$ BMGs changes from crystalline compounds to an icosahedral (I) phase by the partial replacement of Cu with noble metals (NM = Pd, Pt, Ag or Au) [31]. Several studies on I-phase precipitation from the amorphous phase upon annealing have focused on similar Zr-based BMGs with 65–70 at% Zr and 3–10 at% NM. The I-phase precipitation has been interpreted to reflect the generation of Ni-NM atomic pairs with positive heats of mixing, leading to the partial destruction of medium-range-ordered atomic configurations. However, there had been no data on the phase decomposition behavior for Zr-rich BMGs containing much larger amounts of NM.

Recently, it has been reported that the addition of larger amounts of NM causes a distinct change in the primary precipitation phase from I-phase to extremely fine cluster-like precipitates; this can be regarded as the formation of a cluster-like glassy phase [12]. These cluster-like glassy alloys have the following compositional features; (1) consisting of at least four elements (Zr, Al, TM_1 and TM_2), (2) large atomic-size mismatches among the main three elements, Zr, Al and TM, (3) negative heats of mixing among the three elements, (4) large atomic size mismatches between TM_1 and TM_2, and (5) positive heats of mixing between TM_1 and TM_2. The factors (1)–(3) are the same as those for the formation of ordinary BMGs. The additional (4) and (5) factors seem to be essential for the formation of the cluster-like glassy phase. Multicomponent BMGs with these compositional and structural features are termed as PHE BMGs [32].

PHE glassy alloys, $Zr_{65}Al_{7.5}Ni_{10}Cu_{2.5}Ag_{15}$, $Zr_{65}Al_{7.5}Ni_{15}Ag_{12.5}$ and $Zr_{65}Al_{7.5}Co_{12.5}Ag_{15}$ [12, 13] exhibit two exothermic peaks in DSC curves. Figure 5 (a) shows X-ray diffraction patterns of PHE $Zr_{65}Al_{7.5}Co_{27.5-x}Ag_x$ glassy alloys annealed for 3.6 ks at temperatures above T_{x1}. Apart from the x=15 alloy, the patterns retain the broad haloes that are typical for a glassy phase, and no distinct change upon annealing is recognized. In addition, as exemplified for the annealed $Zr_{65}Al_{7.5}Co_{17.5}Ag_{10}$ alloy in Fig. 5 (b)-(e) [13], the TEM data also show the material to be fully amorphous. No appreciable crystalline precipitates are observed, even after annealing for a long time at temperatures well above T_{x1}, indicating that the PHE amorphous alloys have extremely high stability against phase decomposition.

The DSC curves of these annealed cluster-like glassy alloys show only the second exothermic peak [13]. The disappearance of the first exothermic peak indicates that calorimetrically the effect of annealing is equivalent to completion of the first-stage crystallization reaction. There appear to be no earlier reports of this strange phenomenon. The change to the cluster-glass phase also increases the Hv by about 1.5 times as compared with the as-prepared glassy alloys.

The absence of appreciable crystalline phase in the cluster-like glassy phase may be due to extremely sluggish crystal grain growth, implying that the PHE alloys also retain a bulk GFA, as is evident from the formation of the BMG rods with diameters up to several millimeters [11–13]. These BMGs do not exhibit the first-stage exothermic peak, but no appreciable contrast corresponding to a crystalline phase is observed over the transverse cross section, indicating the formation of Zr-based BMGs with higher resistance to crystallization as compared with ordinary BMGs [13].

Summary

Studies on the potential heat-resistant properties of multicomponent Fe- and Zr-based glassy alloys have been reviewed. Fe-Cr-Mo-C-B glassy alloys have high GFA which enables the formation of BMG rods with diameters up to 4 mm, exhibit high mechanical strength and good corrosion resistance. The high GFA has also enabled glassy coatings with a thickness of at least 0.5 mm to be applied to a diverse range of substrates by the high-velocity spray-coating technique. Such a glassy coating has been applied to vessels for melting of lead-free solder liquid, an application which requires elevated-temperature resistance to corrosion and erosion. Novel cluster-like BMGs with significantly enhanced strength were formed after annealing for long holding times at temperatures well above T_{x1} for PHE $Zr_{55–65}Al_{7.5\text{-}10}(TM_1,TM_2)_{27.5–35}$ (TM_1 = Fe,Co,Ni, TM_2 = Cu,Pd,Ag,Au) alloys. Multicomponent Fe-based and PHE BMGs are promising for the future development of heat-resistant structural materials retaining strength at elevated temperature.

References

1. A. Inoue, *Acta Mater* **48**, 279 (2000).
2. W.L. Johnson, *MRS Bull.* **24**, 42 (1999).
3. A.L. Greer, *Science* **267**, 1947 (1995).
4. C. Suryanarayana, A. Inoue, *Bulk Metallic Glasses*, Second Ed., (CRC Press, Boca Raton, FL, 2017).
5. W.M. Yang, H.S. Liu, X.J. Liu, G.X. Chen, C.C. Dun, Y.C. Zhao, Q.K. Man, C.T. Chang, B.L. Shen, A. Inoue, R.W. Li, J.Z. Jiang, *J Appl. Phys.* **116**, 123512 (2014).
6. L. Ma, L. Wang, T. Zhang, A. Inoue, *Mater. Trans.* **43**, 277 (2002).
7. B. Cantor, I.T.H. Chang, P. Knight, A.J.B. Vincent, *Mater. Sci. Eng. A* **375–377**, 213 (2004).
8. J.W. Yeh, *Ann. Chim. Sci. Mater.* **31**, 633 (2006).
9. Y. Zhang, Y.J. Zhou, J.P. Lin, G.L. Chen, P.K. Liaw, *Adv. Eng. Mater.* **10**, 534 (2008).
10. B.S. Murty, J.W. Yeh, S. Ranganathan, *High-Entropy Alloys*, (Butterworth-Heinemann, Oxford, UK, 2014).
11. A. Inoue, Z. Wang, D.V. Louzguine-Luzgin, Y. Han, F.L. Kong, E. Shalaan, F. Al-Marzouki, *J. Alloy. Comp.* **638**, 197 (2015).
12. M.M. Li, A. Inoue, Y. Han, F.L. Kong, S.L. Zhu, E. Shalaan, F. Al-Marzouki, *J. Alloy. Comp.* **735**, 1712 (2018).
13. Y.N. Guo, A. Inoue, Y. Han, F.L. Kong, B. Feng, S.L. Zhu, Y. Ikuhara, *J. Alloy. Comp.* **783**, 545 (2019).
14. W. Klement, R.H. Willens, P. Duwez, *Nature* **187**, 869 (1960).
15. A. Inoue, T. Masumoto, S. Arakawa, T. Iwadachi, *Trans. Jap. Inst. Met.* **19**, 303 (1978).
16. A. Inoue, T. Masumoto, S. Arakawa, T. Iwadachi, in *Rapidly Quenched Metals III*, B. Cantor, Ed. (Metals Society, London, 1978), p. 265.
17. A. Inoue, S. Arakawa, T. Masumoto, *Trans. Jap. Inst. Met.* **19**, 11 (1978).
18. A. Inoue, L. Arnberg, M. Oguchi, U. Backmark, N. Bäckström, T. Masumoto, *Mater. Sci. Eng.* **95**, 101 (1987).
19. A. Inoue, L. Arnberg, M. Oguchi, U. Backmark, N. Backstrom, T. Masumoto, *Trans. Iron Steel Inst. Jap.* **28**, 7 (1988).
20. L. Arnberg, E. Larsson, S. Savage, A. Inoue, S. Yamaguchi, M. Kikuchi, *Mater. Sci. Eng. A* **133**, 288 (1991).
21. A. Inoue, Y. Shinohara, J.S. Gook, *Mater. Trans. JIM* **36**, 1427 (1995).
22. S.J. Pang, T. Zhang, K. Asami, A. Inoue *Acta Mater.* **50**, 489 (2002).
23. S. Pang, T. Zhang, K. Asami, A. Inoue, *J. Mater. Res.* **17**, 701 (2002).
24. V. Ponnambalam, S.J. Poon, G.J. Shiflet, *J. Mater. Res.* **19**, 1320 (2004).
25. Z.P. Lu, C.T. Liu, J.R. Thompson, W.D. Porter, *Phys. Rev. Lett.* **92**, 245503 (2004).
26. K. Amiya, A. Inoue, *Rev. Adv. Mater. Sci.* **18**, 27 (2008).
27. A. Hirata, Y. Hirotsu, K. Amiya, A. Inoue, *Phys. Rev. B* **78**, 144205 (2008).
28. D.V. Louzguine-Luzgin, A.I. Bazlov, S.V. Ketov, A.L. Greer, A. Inoue, *Acta Mater.* **82**, 396 (2015).

29. H.G. Kim, K. Nakata, T. Tsumura, M. Sugiyama, T. Igarashi, M. Fukumoto, H. Kimura, A. Inoue, *Mater. Sci. Forum* **580-582**, 467 (2008).
30. M. Sugiyama, T. Igarashi, T. Okano, H. Kimura, A. Inoue, *Mater. Jap.* **46**, 31 (2007).
31. A. Inoue, T. Zhang, J. Saida, M. Matsushita, M.W. Chen, T. Sakurai, *Mater. Trans. JIM* **40**, 1181 (1999).
32. A. Inoue, F.L. Kong, S.L. Zhu, F. Al-Marzouki, *J. Alloy. Comp.* **707**, 12 (2017).

Figure Captions

Figure 1. Glass formation range for as-spun Fe-Cr-Mo-C-B alloys and compositional dependences of T_g and T_x of the glassy alloys.

Figure 2. (a) Maximum diameters for Fe-Cr-Mo-C-B and Fe-Cr-Mo-C-B-Ln BMG rods prepared by copper mold casting, and (b) T_g, T_x, Hv and fracture strength of their BMGs.

Figure 3. (a) Cross-sectional structure, (b) corrosive potential and anodic current density curve, (c) image after repeated bending deformation of a FeCrMoCB glassy coating prepared by high-velocity oxy-fuel (HVOF) spray coating, and (d) the appearance metallic-glass coatings sprayed on to aluminum pipes.

Figure 4. (a) Inner surface appearance of a vessel for melting lead-free solder after six months of use; the stainless-steel vessel in this case has a $Fe_{43}Cr_{16}Mo_{16}C_{15}B_{10}$ glassy coating on the inner surface. (b) Surface degradation of the best-performing uncoated stainless-steel vessel after only 50 days of use.

Figure 5. (a) X-ray diffraction patterns of $Zr_{65}Al_{7.5}Co_{27.5-x}Ag_x$ (x = 5–20 at%) melt-spun ribbons, (b) TEM bright-field image, (c) selected-area electron diffraction pattern, (d) HRTEM image and (e) nanobeam diffraction pattern of $Zr_{65}Al_{7.5}Co_{17.5}Ag_{10}$ alloy annealed for 7.2 ks at 713 K, a temperature above the first exothermic peak in DSC traces.

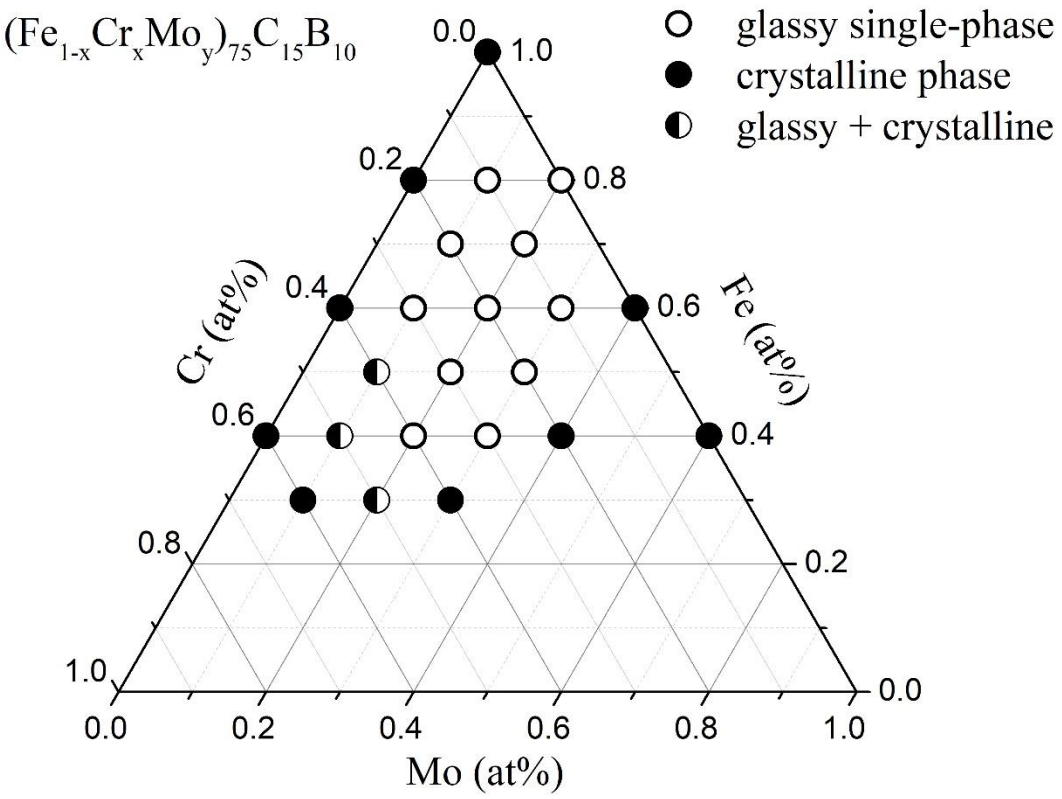

Figure 1

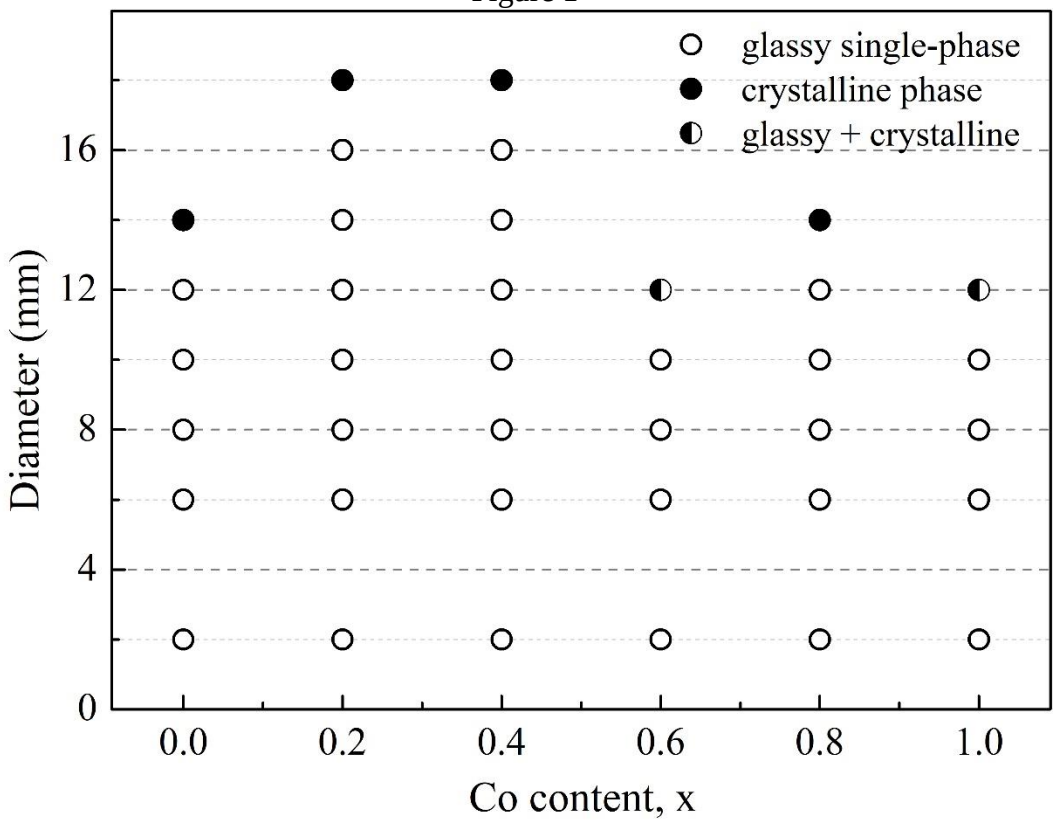

Figure 2

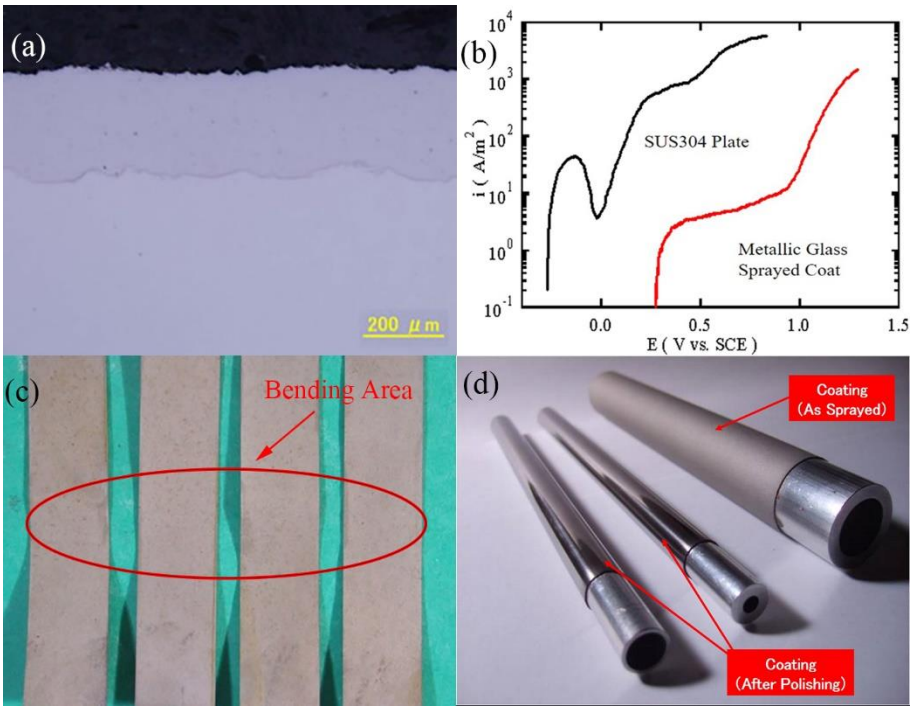

Figure 3

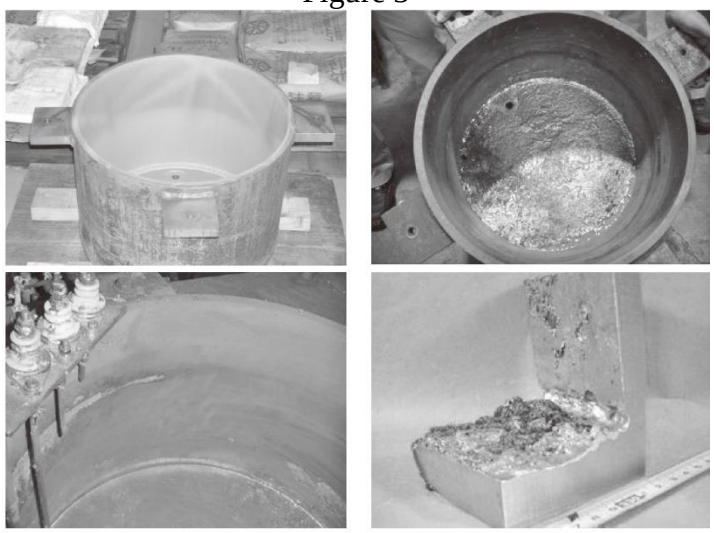

Figure 4

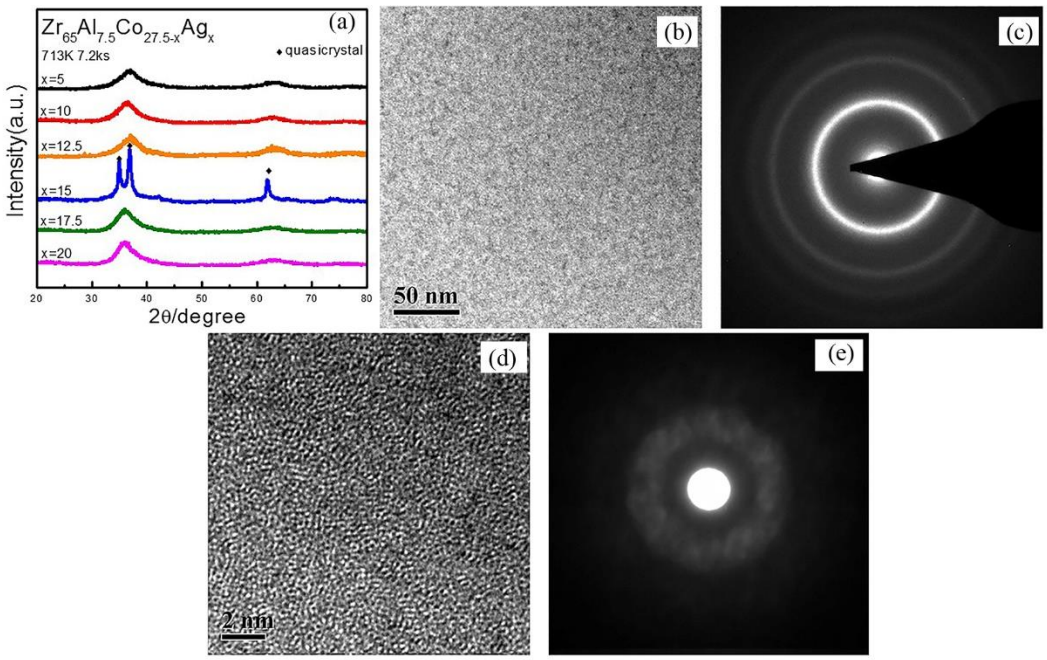

Figure 5

Table 1. Results of wear tests on metallic glass coating, hard chromium plating and CrN coating.

Coating Material	Weight of Specimen		Wear Loss
	(a) Before /g	(b) After /g	(b–a) /g
Metallic glass coating	74.04	74.03	0.01
Hard chromium plating	73.48	73.07	0.41
CrN coating	71.02	70.91	0.11